Acta Cryst E
CRYSTALLOGRAPHIC COMMUNICATIONS
ISSN 2056-9890

Crystal structure and Hirshfeld surface analysis of (*E*)-1-(4-chlorophenyl)-2-[2,2-dichloro-1-(4-fluorophenyl)ethenyl]diazene

Namiq Q. Shikhaliyev,[a] Sevim Türktekin Çelikesir,[b] Mehmet Akkurt,[b] Khanim N. Bagirova,[a] Gulnar T. Suleymanova[a] and Flavien A. A. Toze[c]*

[a]Organic Chemistry Department, Baku State University, Z. Xalilov str. 23, Az, 1148 Baku, Azerbaijan, [b]Department of Physics, Faculty of Sciences, Erciyes University, 38039 Kayseri, Turkey, and [c]Department of Chemistry, Faculty of Sciences, University of Douala, PO Box 24157, Douala, Republic of Cameroon. *Correspondence e-mail: toflavien@yahoo.fr

Received 4 March 2019
Accepted 15 March 2019

Edited by H. Ishida, Okayama University, Japan

Keywords: crystal structure; 4-chlorophenyl; 4-fluorophenyl; face-to-face π-π stacking interaction; Hirshfeld surface analysis.

CCDC reference: 1882554

Supporting information: this article has supporting information at journals.iucr.org/e

In the title compound, $C_{14}H_8Cl_3FN_2$, the planes of the 4-fluorophenyl ring and the 4-chlorophenyl ring make a dihedral angle of 56.13 (13)°. In the crystal, molecules are stacked in a column along the *a* axis *via* a weak C—H···Cl hydrogen bond and face-to-face π–π stacking interactions [centroid–centroid distances = 3.8615 (18) and 3.8619 (18) Å]. The crystal packing is further stabilized by short Cl···Cl contacts. The Hirshfeld surface analysis of the crystal structure indicates that the most important contributions for the crystal packing are from Cl···H/H···Cl (31.2%), H···H (14.8%), C···H/H···C (14.0%), F···H/H···F (12.8%), C···C (9.0%) and Cl···Cl (6.7%) interactions.

1. Chemical context

Azo compounds provide ubiquitous motifs in synthetic chemistry and are widely used as organic dyes, indicators, molecular switches, pigments, ligands, food additives, radical reaction initiators, therapeutic agents *etc.* (Gurbanov *et al.*, 2017; Maharramov *et al.*, 2018; Mahmudov *et al.*, 2019). Azo dyes are also convenient model compounds to study both *E*/*Z* isomerization and noncovalent interactions (Mahmudov *et al.*, 2015; Shixaliyev *et al.*, 2018). Thus, decorating the structure of dyes with tailored functionalities (noncovalent bond donor centres) can be a pivotal strategy for controlling and tuning their functional properties (Mahmudov *et al.*, 2017; Zubkov *et al.*, 2018). Herein we report the molecular structure and noncovalent interactions in the title compound.

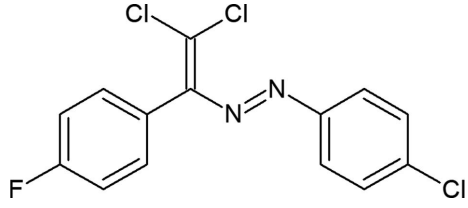

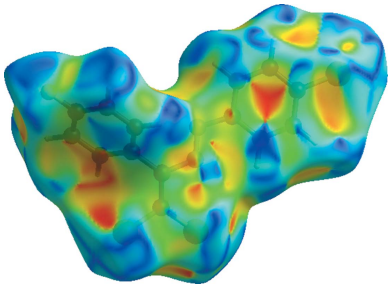

2. Structural commentary

The molecular conformation of the title compound is not planar (Fig. 1); the planes of the 4-fluorophenyl ring and the 4-chlorophenyl ring form a dihedral angle of 56.13 (13)°. The C4—C3—C1—N1, C8—C3—C1—C2, C3—C1—C2—Cl1, C3—C1—C2—Cl2, N1—C1—C2—Cl1, N1—C1—C2—Cl2, C1—N1—N2—C9 and N1—N2—C9—C14 torsion angles are 48.4 (4), 49.2 (4), −1.9 (4), 177.94 (19), 177.14 (18), −3.0 (3), 179.2 (2) and 175.9 (2)°, respectively.

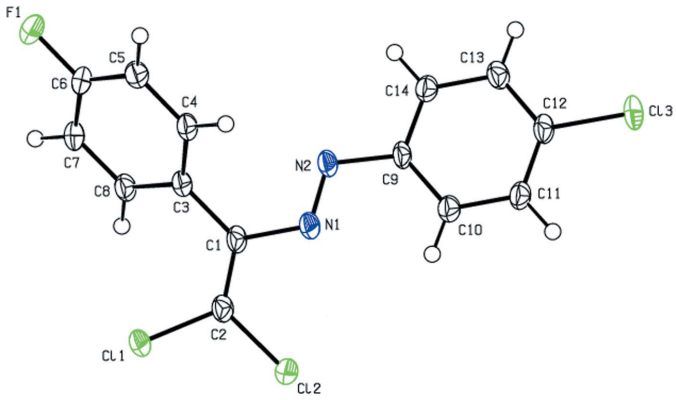

Figure 1
The molecular structure of the title compound, with the atom-labelling scheme and 50% probability displacement ellipsoids.

3. Supramolecular features and Hirshfeld surface analysis

In the crystal, molecules are linked by a weak C—H···Cl hydrogen bond (Table 1), forming a column along the *a* axis (Figs. 2 and 3). The column is further stabilized by face-to-face π–π stacking interactions; the centroid–centroid distances between the adjacent C3–C8 rings and between the adjacent C9–C14 rings are 3.8615 (18) and 3.8619 (18) Å, respectively. Moreover, the columns are linked by intermolecular Cl···Cl short contacts, with distances of 3.3756 (11) and 3.3841 (11) Å (Table 2), forming a layer parallel to the *bc* plane (Fig. 2).

Hirshfeld surfaces and fingerprint plots were generated for the title compound using *CrystalExplorer* (McKinnon *et al.*, 2007). The Hirshfeld surface mapped over $d_{\rm norm}$ using a standard surface resolution with a fixed colour scale of −0.0941 (red) to 1.4174 a.u. (blue) is shown in Fig. 4. This plot was generated to quantify and visualize the intermolecular interactions and to explain the observed crystal packing. The dark-red spots on the $d_{\rm norm}$ surface arise as a result of the C—H···Cl interaction and short interatomic contacts (Tables 1 and 2), while the other weaker intermolecular interactions appear as light-red spots. The shape index of the Hirshfeld surface is a tool to visualize the π–π stacking by the presence of adjacent red and blue triangles; if there are no adjacent red and/or blue triangles, then there are no π–π interactions. Fig. 5 clearly suggests that there are π–π interactions in the title compound.

The percentage contributions of the various contacts to the total Hirshfeld surface are shown in the 2D fingerprint plots in Fig. 6. The reciprocal Cl···H/H···Cl interactions appear as two symmetrical broad wings with $d_{\rm e} + d_{\rm i} \simeq 2.7$ Å and contribute 31.2% to the Hirshfeld surface (Fig. 6*b*). The H···H interactions appear in the middle of the scattered

Table 1
Hydrogen-bond geometry (Å, °).

D—H···*A*	*D*—H	H···*A*	*D*···*A*	*D*—H···*A*
C8—H8···Cl1$^{\rm i}$	0.95	2.81	3.634 (3)	146

Symmetry code: (i) $x-1, y, z$.

Table 2
Summary of short interatomic contacts (Å) in the title compound.

Contact	Distance	Symmetry operation
H4···N2	2.67	$1+x, y, z$
Cl1···Cl3	3.3756 (11)	$-x, -\frac{1}{2}+y, \frac{1}{2}-z$
Cl1···Cl3	3.3841 (11)	$1-x, -\frac{1}{2}+y, \frac{1}{2}-z$
Cl2···H14	3.03	$1+x, \frac{1}{2}-y, -\frac{1}{2}+z$
H11···F1	2.81	$x, \frac{1}{2}-y, -\frac{1}{2}+z$
H7···F1	2.67	$1-x, -y, 1-z$
F1···H11	2.84	$1+x, \frac{1}{2}-y, \frac{1}{2}+z$

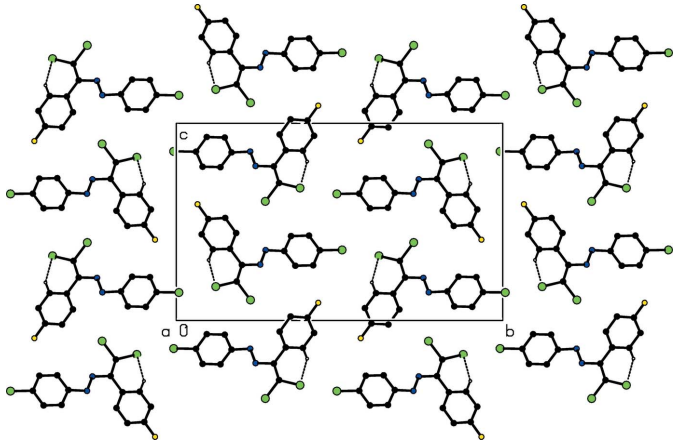

Figure 2
A packing diagram of the title compound, viewed along the *a* axis, showing the C—H···Cl interactions (dashed lines).

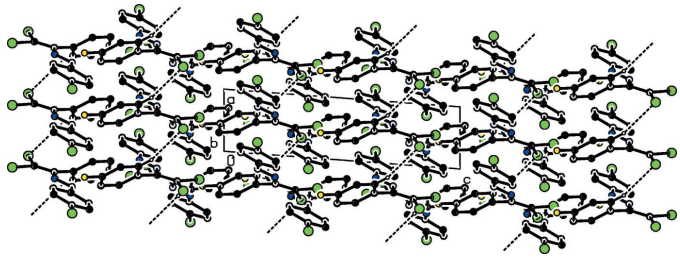

Figure 3
A packing diagram of the title compound, viewed along the *b* axis, showing the C—H···Cl interactions (dashed lines).

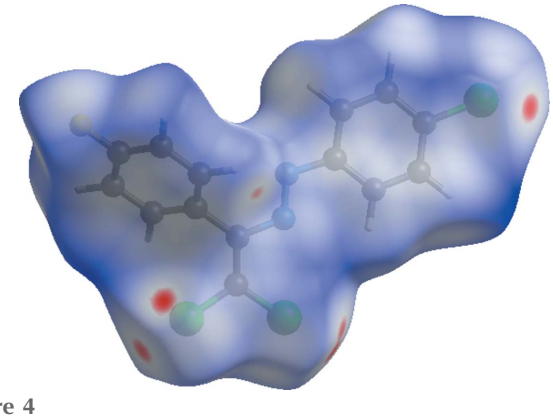

Figure 4
View of the Hirshfeld surface of the title compound plotted over $d_{\rm norm}$ in the range from −0.0941 to 1.4174 a.u.

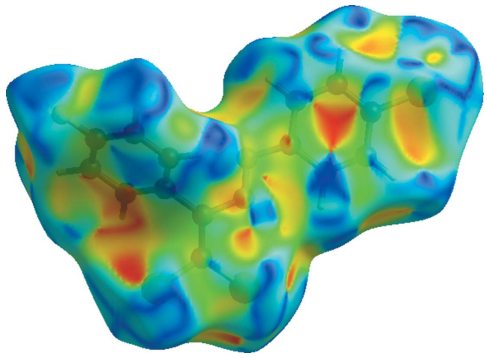

Figure 5
View of the Hirshfeld surface of the title compound plotted over shape index.

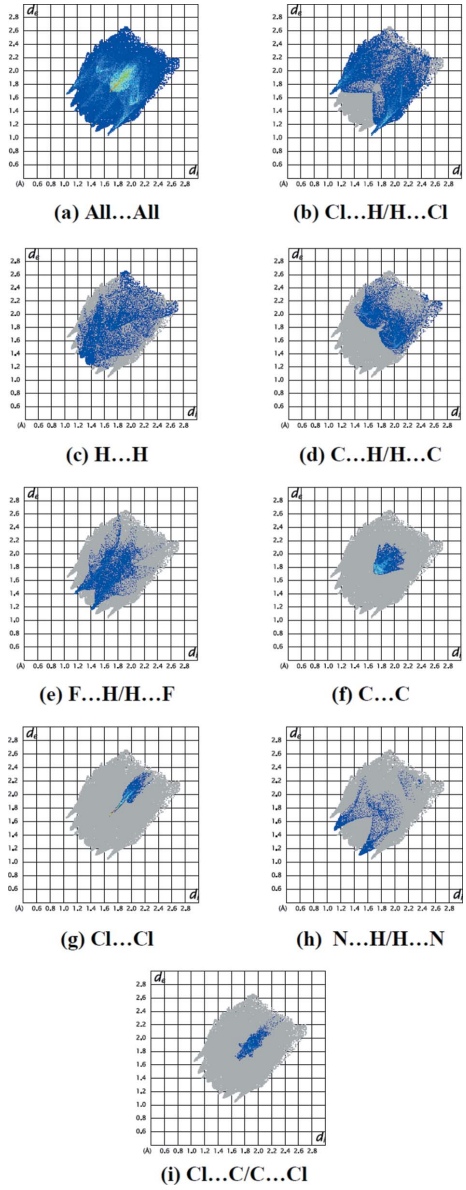

Figure 6
The full 2D fingerprint plots for the title compound, showing (*a*) all interactions, and those delineated into (*b*) Cl···H/H···Cl, (*c*) H···H, (*d*) C···H/H···C, (*e*) F···H/H···F, (*f*) C···C, (*g*) Cl···Cl, (*h*) N···H/H···N and (*i*) Cl···C/C···Cl interactions. The d_i and d_e values are the closest internal and external distances (in Å) from given points on the Hirshfeld surface contacts.

points in the 2D fingerprint plots, with an overall contribution to the Hirshfeld surface of 14.8% (Fig. 6*c*). The C···H/H···C interactions, with a 14.0% contribution, are present as bump symmetrical spikes at diagonal axes (Fig. 6*d*). The F···H/H···F interactions, with a 12.8% contribution, are present as sharp symmetrical spikes at diagonal axes $d_e + d_i \simeq 2.55$ Å (Fig. 6*e*). The C···C interactions appear in the middle of the scattered points in the 2D fingerprint plots with an overall contribution to the Hirshfeld surface of 9.0% (Fig. 6*f*). The small percentage contributions from the other different interatomic contacts to the Hirshfeld surfaces are as follows: Cl···Cl (6.7%) (Fig. 6*g*), N···H/H···N (3.4%) (Fig. 6*h*), Cl···C/C···Cl (3.1%) (Fig. 6*i*), N···C/C···N (2.8%), N···N (1.0%), Cl···N/N···Cl (0.8%), F···F (0.4%) and F···C/C···F (0.1%). Hirshfeld surface representations with the function d_{norm} plotted onto the surface for Cl···H/H···Cl, H···H,

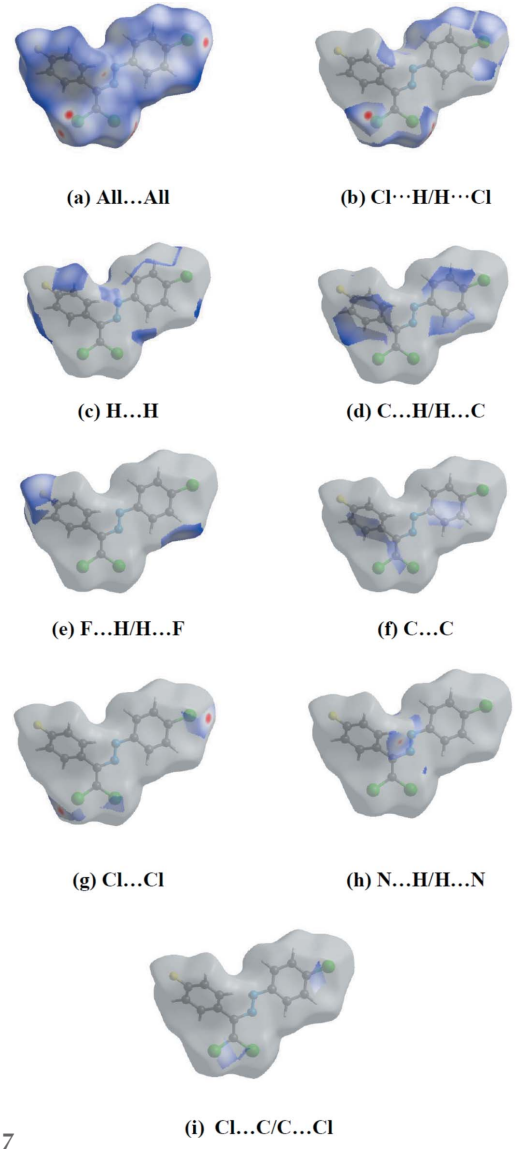

Figure 7
Hirshfeld surface representations with the function d_{norm} plotted onto the surface for (*a*) all interactions, (*b*) Cl···H/H···Cl, (*c*) H···H, (*d*) C···H/H···C, (*e*) F···H/H···F, (*f*) C···C, (*g*) Cl···Cl, (*h*) N···H/H···N and (*i*) Cl···C/C···Cl interactions.

C···H/H···C, F···H/H···F, C···C, Cl···Cl, N···H/H···N and Cl···C/C···Cl interactions are shown in Fig. 7. The large number of Cl···H/H···Cl, H···H, C···H/H···C, F···H/H···F and C···C interactions suggest that van der Waals interactions and hydrogen bonding play the major roles in the crystal packing (Hathwar *et al.*, 2015).

4. Database survey

A search of the Cambridge Structural Database (CSD, Version 5.40, November 2018; Groom *et al.*, 2016) for structures having an (*E*)-1-(2,2-dichloro-1-phenylvinyl)-2-phenyldiazene unit gave 18 hits. Three compounds closely resemble the title compound, *viz*. 1-[2,2-dichloro-1-(4-nitrophenyl)ethenyl]-2-(4-fluorophenyl)diazene (CSD refcode XIZREG; Atioğlu *et al.*, 2019), 1,1′-[methylenebis(4,1-phenylene)]bis[(2,2-dichloro-1-(4-nitrophenyl)ethenyl]diazene (LEQXIR; Shixaliyev *et al.*, 2018) and 1,1′-[methylenebis(4,1-phenylene)]bis{[2,2-dichloro-1-(4-chlorophenyl)ethenyl]diazene} (LEQXOX; Shixaliyev *et al.*, 2018). In XIZREG (Atioğlu *et al.*, 2019), molecules are linked by a C—H···O hydrogen bond into a zigzag chain running along the *c* axis. The crystal packing is further stabilized by C—Cl···π, C—F···π and N—O···π interactions. In the crystal of LEQXIR, C—H···N and C—H···O hydrogen bonds and Cl···O contacts were found, and in LEQXOX, C—H···N and Cl···Cl contacts were observed.

5. Synthesis and crystallization

This dye was synthesized according to a reported method (Shixaliyev *et al.*, 2018). A 20 ml screw-necked vial was charged with dimethyl sulfoxide (10 ml), (*E*)-1-(4-chlorophenyl)-2-(4-fluorobenzylidene)hydrazine (248 mg, 1 mmol), tetramethylethylenediamine (295 mg, 2.5 mmol), CuCl (2 mg, 0.02 mmol) and CCl_4 (20 mmol, 10 equiv.). After 1–3 h (until thin-layer chromatography analysis showed complete consumption of the corresponding Schiff base), the reaction mixture was poured into a ~0.01 *M* solution of HCl (100 ml, ~pH = 2–3) and extracted with dichloromethane (3 × 20 ml). The combined organic phase was washed with water (3 × 50 ml), brine (30 ml), dried over anhydrous Na_2SO_4 and concentrated *in vacuo* with a rotary evaporator. The residue was purified by column chromatography on silica gel using appropriate mixtures of hexane and dichloromethane (3:1–1:1 *v*/*v*).

Red solid (yield 46%); m.p. 340–338 K. Analysis calculated (%) for $C_{14}H_8Cl_3FN_2$: C 51.02, H 2.45, N 8.50; found: C 49.95, H 2.43, N 8.47. ^{1}H NMR (300 MHz, $CDCl_3$): δ 7.15-7.17 (*m*, 4H), 7.42–7.45 (*d*, 2H, *J* = 9.21 Hz), 7.73–7.75 (*d*, 2H, *J* = 6.04 Hz). ^{13}C NMR (75 MHz, $CDCl_3$): δ 115.29, 115.58, 124.49, 127.46, 129.37, 130.43, 131.88, 131.99, 137.73, 151.13. ESI-MS: *m*/*z*: 330.44 $[M + H]^+$.

6. Refinement

Crystal data, data collection and structure refinement details are summarized in Table 3. C-bound H atoms were constrained to an ideal geometry, with C—H = 0.95 Å and $U_{iso}(H) = 1.2U_{eq}(C)$. Nine outliers ($\bar{4}$,2,12; $\bar{4}$,1,12; $\bar{3}$,18,11; 2,21,1; $\bar{4}$,3,12; $\bar{3}$,19,10; 0,13,17; $\bar{4}$,4,10; 2,20,0) were omitted in the final cycles of refinement.

Table 3
Experimental details.

Crystal data	
Chemical formula	$C_{14}H_8Cl_3FN_2$
M_r	329.57
Crystal system, space group	Monoclinic, $P2_1/c$
Temperature (K)	100
a, *b*, *c* (Å)	3.8617 (8), 24.249 (5), 14.724 (3)
β (°)	94.30 (3)
V (Å^3)	1374.9 (5)
Z	4
Radiation type	Synchrotron, λ = 0.80246 Å
μ (mm^{-1})	0.93
Crystal size (mm)	0.20 × 0.10 × 0.02
Data collection	
Diffractometer	Rayonix SX165 CCD
Absorption correction	Multi-scan (*SCALA*; Evans, 2006)
T_{min}, T_{max}	0.840, 0.970
No. of measured, independent and observed [$I > 2\sigma(I)$] reflections	20761, 2984, 2719
R_{int}	0.115
$(\sin \theta/\lambda)_{max}$ (Å^{-1})	0.640
Refinement	
$R[F^2 > 2\sigma(F^2)]$, $wR(F^2)$, *S*	0.053, 0.142, 1.05
No. of reflections	2984
No. of parameters	182
H-atom treatment	H-atom parameters constrained
$\Delta\rho_{max}$, $\Delta\rho_{min}$ (e Å^{-3})	0.59, −0.72

Computer programs: *Marccd* (Doyle, 2011), *iMosflm* (Battye *et al.*, 2011), *SHELXS97* (Sheldrick, 2008), *SHELXL2018* (Sheldrick, 2015), *ORTEP-3 for Windows* (Farrugia, 2012) and *PLATON* (Spek, 2009).

Funding information

Funding for this research was provided by: Science Development Foundation under the President of the Republic of Azerbaijan (grant No. EİF/MQM/Elm-Tehsil-1-2016-1(26)-71/06/4).

References

Atioğlu, Z., Akkurt, M., Shikhaliyev, N. Q., Suleymanova, G. T., Bagirova, K. N. & Toze, F. A. A. (2019). *Acta Cryst.* E**75**, 237–241.
Battye, T. G. G., Kontogiannis, L., Johnson, O., Powell, H. R. & Leslie, A. G. W. (2011). *Acta Cryst.* D**67**, 271–281.
Doyle, R. A. (2011). *Marccd software manual*. Rayonix LLC, Evanston, USA.
Evans, P. (2006). *Acta Cryst.* D**62**, 72–82.
Farrugia, L. J. (2012). *J. Appl. Cryst.* **45**, 849–854.
Groom, C. R., Bruno, I. J., Lightfoot, M. P. & Ward, S. C. (2016). *Acta Cryst.* B**72**, 171–179.
Gurbanov, A. V., Mahmudov, K. T., Kopylovich, M. N., Guedes da Silva, M. F. C., Sutradhar, M., Guseinov, F. I., Zubkov, F. I., Maharramov, A. M. & Pombeiro, A. J. L. (2017). *Dyes Pigments*, **138**, 107–111.
Hathwar, V. R., Sist, M., Jørgensen, M. R. V., Mamakhel, A. H., Wang, X., Hoffmann, C. M., Sugimoto, K., Overgaard, J. & Iversen, B. B. (2015). *IUCrJ*, **2**, 563–574.

Maharramov, A. M., Shikhaliyev, N. Q., Suleymanova, G. T., Gurbanov, A. V., Babayeva, G. V., Mammadova, G. Z., Zubkov, F. I., Nenajdenko, V. G., Mahmudov, K. T. & Pombeiro, A. J. L. (2018). *Dyes Pigments*, **159**, 135–141.

Mahmudov, K. T., Guedes da Silva, M. F. C., Sutradhar, M., Kopylovich, M. N., Huseynov, F. E., Shamilov, N. T., Voronina, A. A., Buslaeva, T. M. & Pombeiro, A. J. L. (2015). *Dalton Trans.* **44**, 5602–5610.

Mahmudov, K. T., Gurbanov, A. V., Guseinov, F. I. & Guedes da Silva, M. F. C. (2019). *Coord. Chem. Rev.* **387**, 32–46.

Mahmudov, K. T., Kopylovich, M. N., Guedes da Silva, M. F. C. & Pombeiro, A. J. L. (2017). *Coord. Chem. Rev.* **345**, 54–72.

McKinnon, J. J., Jayatilaka, D. & Spackman, M. A. (2007). *Chem. Commun.* pp. 3814–3816.

Sheldrick, G. M. (2008). *Acta Cryst.* A**64**, 112–122.

Sheldrick, G. M. (2015). *Acta Cryst.* C**71**, 3–8.

Shixaliyev, N. Q., Ahmadova, N. E., Gurbanov, A. V., Maharramov, A. M., Mammadova, G. Z., Nenajdenko, V. G., Zubkov, F. I., Mahmudov, K. T. & Pombeiro, A. J. L. (2018). *Dyes Pigments*, **150**, 377–381.

Spek, A. L. (2009). *Acta Cryst.* D**65**, 148–155.

Zubkov, F. I., Mertsalov, D. F., Zaytsev, V. P., Varlamov, A. V., Gurbanov, A. V., Dorovatovskii, P. V., Timofeeva, T. V., Khrustalev, V. N. & Mahmudov, K. T. (2018). *J. Mol. Liq.* **249**, 949–952.

supporting information

Acta Cryst. (2019). E**75**, 465-469 [https://doi.org/10.1107/S2056989019003657]

Crystal structure and Hirshfeld surface analysis of (*E*)-1-(4-chlorophenyl)-2-[2,2-dichloro-1-(4-fluorophenyl)ethenyl]diazene

Namiq Q. Shikhaliyev, Sevim Türktekin Çelikesir, Mehmet Akkurt, Khanim N. Bagirova, Gulnar T. Suleymanova and Flavien A. A. Toze

Computing details

Data collection: *Marccd* (Doyle, 2011); cell refinement: *iMosflm* (Battye *et al.*, 2011); data reduction: *iMosflm*; program(s) used to solve structure: *SHELXS97* (Sheldrick, 2008); program(s) used to refine structure: *SHELXL2018* (Sheldrick, 2015); molecular graphics: *ORTEP-3 for Windows* (Farrugia, 2012); software used to prepare material for publication: *PLATON* (Spek, 2009).

(*E*)-1-(4-Chlorophenyl)-2-[2,2-dichloro-1-(4-fluorophenyl)ethenyl]\ diazene

Crystal data

$C_{14}H_8Cl_3FN_2$
M_r = 329.57
Monoclinic, $P2_1/c$
a = 3.8617 (8) Å
b = 24.249 (5) Å
c = 14.724 (3) Å
β = 94.30 (3)°
V = 1374.9 (5) Å^3
Z = 4
F(000) = 664
D_x = 1.592 Mg m^{-3}
Synchrotron radiation, λ = 0.80246 Å
Cell parameters from 600 reflections
θ = 3.3–30.0°
μ = 0.93 mm^{-1}
T = 100 K
Plate, orange
0.20 × 0.10 × 0.02 mm

Data collection

Rayonix SX165 CCD diffractometer
/f scan
Absorption correction: multi-scan (*Scala*; Evans, 2006)
T_{min} = 0.840, T_{max} = 0.970
20761 measured reflections
2984 independent reflections
2719 reflections with $I > 2\sigma(I)$
R_{int} = 0.115
θ_{max} = 30.9°, θ_{min} = 3.3°
$h = -4 \rightarrow 4$
$k = -30 \rightarrow 31$
$l = -18 \rightarrow 18$

Refinement

Refinement on F^2
Least-squares matrix: full
$R[F^2 > 2\sigma(F^2)]$ = 0.053
$wR(F^2)$ = 0.142
S = 1.05
2984 reflections
182 parameters
0 restraints
Primary atom site location: difference Fourier map
Secondary atom site location: difference Fourier map
Hydrogen site location: inferred from neighbouring sites
H-atom parameters constrained
$w = 1/[\sigma^2(F_o^2) + (0.0557P)^2 + 1.092P]$ where $P = (F_o^2 + 2F_c^2)/3$

$(\Delta/\sigma)_{max}$ = 0.001
$\Delta\rho_{max}$ = 0.59 e Å^{-3}
$\Delta\rho_{min}$ = −0.72 e Å^{-3}

Extinction correction: SHELXL2018 (Sheldrick, 2015), $Fc^*=kFc[1+0.001xFc^2\lambda^3/\sin(2\theta)]^{-1/4}$
Extinction coefficient: 0.026 (3)

Special details

Geometry. All esds (except the esd in the dihedral angle between two l.s. planes) are estimated using the full covariance matrix. The cell esds are taken into account individually in the estimation of esds in distances, angles and torsion angles; correlations between esds in cell parameters are only used when they are defined by crystal symmetry. An approximate (isotropic) treatment of cell esds is used for estimating esds involving l.s. planes.

Fractional atomic coordinates and isotropic or equivalent isotropic displacement parameters (Å^2)

	x	*y*	*z*	U_{iso}*/U_{eq}
Cl1	0.68912 (17)	0.12097 (2)	0.17209 (4)	0.0265 (2)
Cl2	0.48467 (18)	0.22728 (2)	0.10431 (4)	0.0283 (2)
Cl3	−0.18247 (18)	0.50802 (2)	0.35787 (5)	0.0318 (2)
F1	0.5868 (5)	0.06509 (7)	0.58998 (10)	0.0386 (4)
N1	0.3562 (6)	0.25699 (8)	0.28387 (14)	0.0246 (5)
N2	0.2435 (6)	0.27366 (8)	0.35685 (14)	0.0230 (4)
C1	0.4622 (7)	0.20110 (9)	0.28183 (16)	0.0225 (5)
C2	0.5361 (7)	0.18506 (9)	0.19760 (16)	0.0237 (5)
C3	0.4936 (7)	0.16469 (9)	0.36354 (16)	0.0232 (5)
C4	0.6716 (7)	0.18329 (10)	0.44378 (16)	0.0249 (5)
H4	0.7714	0.2191	0.4459	0.030*
C5	0.7036 (7)	0.14978 (10)	0.52038 (16)	0.0283 (6)
H5	0.8242	0.1622	0.5752	0.034*
C6	0.5558 (8)	0.09804 (10)	0.51483 (17)	0.0287 (6)
C7	0.3803 (7)	0.07791 (10)	0.43694 (17)	0.0280 (5)
H7	0.2840	0.0418	0.4352	0.034*
C8	0.3485 (7)	0.11196 (10)	0.36103 (17)	0.0243 (5)
H8	0.2264	0.0992	0.3067	0.029*
C9	0.1482 (7)	0.33066 (9)	0.35229 (16)	0.0225 (5)
C10	0.1990 (7)	0.36475 (10)	0.27784 (16)	0.0251 (5)
H10	0.3012	0.3504	0.2261	0.030*
C11	0.1000 (7)	0.41943 (10)	0.27997 (16)	0.0257 (5)
H11	0.1332	0.4430	0.2298	0.031*
C12	−0.0490 (7)	0.43956 (10)	0.35640 (17)	0.0246 (5)
C13	−0.0997 (7)	0.40658 (10)	0.43064 (17)	0.0255 (5)
H13	−0.2002	0.4212	0.4824	0.031*
C14	−0.0012 (7)	0.35157 (10)	0.42818 (16)	0.0248 (5)
H14	−0.0358	0.3282	0.4784	0.030*

Atomic displacement parameters (Å^2)

	U^{11}	U^{22}	U^{33}	U^{12}	U^{13}	U^{23}
Cl1	0.0363 (4)	0.0157 (3)	0.0273 (3)	0.0018 (2)	0.0006 (2)	−0.0038 (2)
Cl2	0.0408 (4)	0.0196 (3)	0.0243 (3)	0.0022 (2)	0.0017 (2)	0.0020 (2)
Cl3	0.0384 (4)	0.0125 (3)	0.0442 (4)	0.0020 (2)	0.0011 (3)	0.0002 (2)

F1	0.0622 (12)	0.0241 (8)	0.0290 (8)	0.0040 (8)	−0.0004 (7)	0.0087 (6)
N1	0.0333 (12)	0.0135 (9)	0.0266 (10)	−0.0008 (8)	0.0000 (8)	−0.0019 (7)
N2	0.0292 (11)	0.0128 (9)	0.0269 (10)	0.0004 (8)	0.0008 (8)	−0.0015 (7)
C1	0.0273 (13)	0.0123 (10)	0.0272 (11)	−0.0027 (9)	−0.0017 (9)	−0.0010 (8)
C2	0.0286 (13)	0.0146 (10)	0.0272 (11)	−0.0032 (9)	−0.0019 (9)	−0.0014 (8)
C3	0.0301 (13)	0.0143 (11)	0.0253 (11)	0.0017 (9)	0.0013 (9)	−0.0013 (8)
C4	0.0316 (14)	0.0149 (11)	0.0279 (11)	0.0016 (9)	0.0007 (10)	−0.0005 (9)
C5	0.0361 (15)	0.0214 (12)	0.0267 (11)	0.0039 (10)	−0.0023 (10)	−0.0023 (9)
C6	0.0407 (15)	0.0175 (11)	0.0280 (11)	0.0064 (10)	0.0037 (10)	0.0060 (9)
C7	0.0376 (15)	0.0143 (11)	0.0321 (12)	0.0007 (10)	0.0037 (10)	0.0016 (9)
C8	0.0291 (13)	0.0153 (11)	0.0285 (11)	0.0000 (9)	0.0013 (10)	−0.0017 (9)
C9	0.0288 (13)	0.0112 (10)	0.0269 (11)	0.0003 (9)	−0.0025 (9)	−0.0011 (8)
C10	0.0315 (14)	0.0176 (11)	0.0259 (11)	−0.0001 (9)	−0.0004 (9)	0.0001 (9)
C11	0.0332 (14)	0.0157 (11)	0.0277 (11)	−0.0010 (9)	−0.0020 (10)	0.0022 (9)
C12	0.0286 (13)	0.0132 (11)	0.0312 (12)	−0.0020 (9)	−0.0037 (10)	−0.0005 (9)
C13	0.0302 (13)	0.0165 (11)	0.0292 (11)	−0.0012 (9)	−0.0009 (9)	−0.0037 (9)
C14	0.0319 (14)	0.0175 (11)	0.0243 (11)	−0.0007 (9)	−0.0019 (9)	0.0013 (9)

Geometric parameters (Å, º)

Cl1—C2	1.714 (2)	C6—C7	1.377 (4)
Cl2—C2	1.713 (2)	C7—C8	1.388 (3)
Cl3—C12	1.739 (2)	C7—H7	0.9500
F1—C6	1.363 (3)	C8—H8	0.9500
N1—N2	1.256 (3)	C9—C14	1.391 (3)
N1—C1	1.417 (3)	C9—C10	1.399 (3)
N2—C9	1.431 (3)	C10—C11	1.381 (3)
C1—C2	1.351 (3)	C10—H10	0.9500
C1—C3	1.490 (3)	C11—C12	1.390 (4)
C3—C8	1.395 (3)	C11—H11	0.9500
C3—C4	1.396 (3)	C12—C13	1.380 (3)
C4—C5	1.388 (3)	C13—C14	1.389 (3)
C4—H4	0.9500	C13—H13	0.9500
C5—C6	1.378 (4)	C14—H14	0.9500
C5—H5	0.9500		
N2—N1—C1	116.43 (19)	C8—C7—H7	121.0
N1—N2—C9	112.0 (2)	C7—C8—C3	120.9 (2)
C2—C1—N1	112.1 (2)	C7—C8—H8	119.6
C2—C1—C3	124.1 (2)	C3—C8—H8	119.6
N1—C1—C3	123.8 (2)	C14—C9—C10	120.4 (2)
C1—C2—Cl2	122.99 (19)	C14—C9—N2	115.8 (2)
C1—C2—Cl1	124.22 (18)	C10—C9—N2	123.9 (2)
Cl2—C2—Cl1	112.79 (14)	C11—C10—C9	119.6 (2)
C8—C3—C4	119.3 (2)	C11—C10—H10	120.2
C8—C3—C1	120.9 (2)	C9—C10—H10	120.2
C4—C3—C1	119.8 (2)	C10—C11—C12	119.2 (2)
C5—C4—C3	120.4 (2)	C10—C11—H11	120.4

C5—C4—H4	119.8	C12—C11—H11	120.4
C3—C4—H4	119.8	C13—C12—C11	122.0 (2)
C6—C5—C4	118.3 (2)	C13—C12—Cl3	118.9 (2)
C6—C5—H5	120.9	C11—C12—Cl3	119.10 (18)
C4—C5—H5	120.9	C12—C13—C14	118.7 (2)
F1—C6—C7	118.4 (2)	C12—C13—H13	120.6
F1—C6—C5	118.3 (2)	C14—C13—H13	120.6
C7—C6—C5	123.2 (2)	C13—C14—C9	120.1 (2)
C6—C7—C8	117.9 (2)	C13—C14—H14	119.9
C6—C7—H7	121.0	C9—C14—H14	119.9

C1—N1—N2—C9	179.2 (2)	C5—C6—C7—C8	−0.8 (4)
N2—N1—C1—C2	171.9 (2)	C6—C7—C8—C3	0.7 (4)
N2—N1—C1—C3	−9.0 (4)	C4—C3—C8—C7	−0.3 (4)
N1—C1—C2—Cl2	−3.0 (3)	C1—C3—C8—C7	179.5 (2)
C3—C1—C2—Cl2	177.94 (19)	N1—N2—C9—C14	175.9 (2)
N1—C1—C2—Cl1	177.14 (18)	N1—N2—C9—C10	−4.5 (4)
C3—C1—C2—Cl1	−1.9 (4)	C14—C9—C10—C11	0.0 (4)
C2—C1—C3—C8	−49.2 (4)	N2—C9—C10—C11	−179.6 (2)
N1—C1—C3—C8	131.8 (3)	C9—C10—C11—C12	0.0 (4)
C2—C1—C3—C4	130.5 (3)	C10—C11—C12—C13	0.3 (4)
N1—C1—C3—C4	−48.4 (4)	C10—C11—C12—Cl3	−178.57 (19)
C8—C3—C4—C5	−0.1 (4)	C11—C12—C13—C14	−0.6 (4)
C1—C3—C4—C5	−179.9 (2)	Cl3—C12—C13—C14	178.31 (19)
C3—C4—C5—C6	0.0 (4)	C12—C13—C14—C9	0.5 (4)
C4—C5—C6—F1	−180.0 (2)	C10—C9—C14—C13	−0.2 (4)
C4—C5—C6—C7	0.4 (4)	N2—C9—C14—C13	179.4 (2)
F1—C6—C7—C8	179.6 (2)		

Hydrogen-bond geometry (Å, º)

D—H···*A*	*D*—H	H···*A*	*D*···*A*	*D*—H···*A*
C8—H8···Cl1^{i}	0.95	2.81	3.634 (3)	146

Symmetry code: (i) $x-1$, y, z.